Damage production in nanoparticles under light ion irradiation

T. T. Järvi,* A. Kuronen, and K. Nordlund
Department of Physics, University of Helsinki, P.O. Box 43, FI-00014 Helsinki, Finland

K. Albe
Institut für Materialwissenschaft, Technische Universität Darmstadt, Petersenstr. 23, D-64287 Darmstadt, Germany
(Received 17 June 2009; revised manuscript received 3 August 2009; published 6 October 2009)

Modifying the properties of nanoparticles by ion irradiation leads to sputtering and defect production, possibly enhanced by the high surface-to-volume ratio of the irradiated objects. By molecular-dynamics simulations, we address the size dependence of platinum nanoparticles' response to light ion irradiation and show that in contrast to irradiation by heavier ions the sputtering yield does *not* depend on the particle size. In contrast, very high vacancy concentrations can be obtained in nanoparticles, the maximal concentration depending on the particle size. The evolution of vacancy concentration and sputtering upon irradiation are rationalized in terms of a kinetic model based on single knock-on events.

DOI: 10.1103/PhysRevB.80.132101 PACS number(s): 61.80.Az, 61.46.Df, 61.82.Bg

In recent years, there have been considerable efforts to use ion irradiation as a tool for modifying the properties of nanoparticles. One example is that the chemical ordering of FePt nanoparticles was enhanced using He irradiation.[1] Recently it was also discovered that the structure and morphology of FePt and CuAu nanoparticles can be modified using light ion irradiation,[2–4] namely, twinned particles turn single crystalline under He irradiation. This effect was proposed to arise from the easier amorphizability of alloyed particles compared to bulk systems.[3] Ion irradiation has also been shown to provide a means to densify porous cluster-assembled films without significantly increasing the grain size.[5] Thus, irradiation is turning out to be a very promising tool for obtaining nanoparticles in phases that are hard or impossible to obtain by other means. It is also worth mentioning that sputtering processes occur in interstellar dust.[6]

Despite the importance of the subject, few studies have systematically looked at the irradiation response of nanoparticles. (Note that we restrict the discussion here to supported or free particles, not particles embedded in solid matrices, for which a lot of work has been done.[7]) The high surface-to-volume ratio was shown to increase sputtering yields dramatically for 16–64 keV Ga and Au irradiation of Au particles of different sizes.[8,9] For particles irradiated in vacuum or on substrates that conduct heat poorly, evaporative sputtering should also be possible,[10] and it was also shown that for particles in vacuum, irradiation could result in a partly molten particle, the solid part of which underwent a structural transition while floating in vacuum.[11]

In a previous work,[8] we studied the sputtering yield of gold clusters under cascade-producing irradiation (25 keV Ga ions) as a function of cluster size and showed that it could be explained by traditional linear cascade sputtering models. In this study, we address the question of size dependence of sputtering under irradiation that is in the single knock-on regime, namely, irradiation of Pt particles under 3 keV helium bombardment. This is the type of irradiation that is used to enhance chemical ordering in $L1_0$ nanoparticles such as FePt and CuAu.

In the following, we outline the technical detail of our simulations. The interatomic interactions were described by an analytic bond-order potential[12] that was, at short distances, smoothly joined to a pair interaction calculated using the Dmol package. The universal repulsive Ziegler-Biersack-Littmark potential[13] was used for the ion-platinum interaction. Inelastic energy losses due to electronic stopping were included via a friction term in the equations of motion of all atoms with kinetic energy higher than 5 eV.[13] For technical reasons, the stopping was also applied somewhat outside the nanoparticle but this amounted on average to less than ~1% of the total stopping for the incoming ion.

For simulating impacts of helium ions on the nanoparticles, the particles were placed in vacuum after relaxing them to 0 K. Truncated octahedral particles (the ground state for Pt because of the high-stacking fault energy) from ~400 to ~4000 atoms in size (from ~2 nm to ~5 nm in diameter) were chosen as targets. The particles were randomly rotated and bombarded with an impact parameter chosen randomly inside a radius, which is given by a cylinder wrapped around the cluster. This procedure caused some ions to miss the target, but the fraction of missed ions was found to be negligible. After each helium impact, the particle was cooled back to 0 K, and the next impact was started. A single cumulative run was made for each particle size and it was assumed that the large number of irradiation events with random impact parameters would suffice for statistical averaging.

The vacancy production was obtained by searching for free volume in the system, in the form of spheres with a radius of 0.8 times the nearest-neighbor (NN) distance, that is, ~2.2 Å. After analyzing all vacancies a clustering algorithm was used to identify and remove the largest vacancy cluster corresponding to vacuum outside the nanoparticle. This method provided a robust way of detecting vacancies while handling surface roughness automatically. The vacancy concentration was calculated as the number of vacancies per atom. The sputtering yield was also determined using a clustering algorithm.

The rapid quenching between each ion impact ignores thermally activated defect migration, but note that for platinum, the vacancy migration energy is very high, around 1.5 eV.[14,15] Thus vacancies are expected to be immobile during

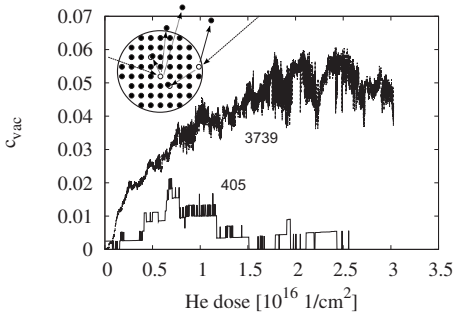

FIG. 1. Concentration of vacancies as a function of helium dose for particles of 405 and 3739 atoms in size. The inset shows the different processes taken into account in the kinetic model.

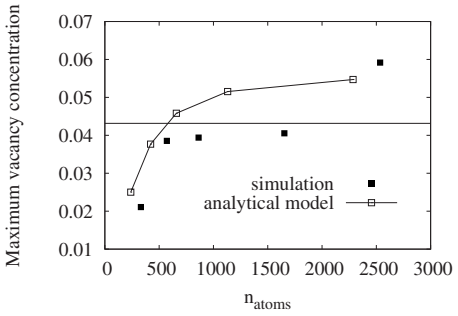

FIG. 2. Maximum vacancy concentration as a function of the nanoparticle size at which it was obtained. The horizontal line shows the result for a bulk surface.

irradiation and interstitials are mostly sputtered because of the closeby nanoparticle surfaces.

To compare to bulk behavior, we also irradiated a bulk (111) surface sample. These simulations were otherwise as described above, except the system was taken periodic in the lateral directions and temperature control was applied at the periodic borders and at the bottom of the cell.

Helium irradiation was found to have a similar effect on particles of all sizes. Initially, the vacancy concentration rises quickly, as shown in Fig. 1. After reaching a maximal value at a concentration of a few percent, it remains constant on average, fluctuating heavily. This is because vacancy production and recombination rates reach a balance. Still increasing the dose leads to a decline in the number of vacancies due to the particle getting smaller by sputtering. For the largest particle sizes such as the larger particle in Fig. 1, the decrease in concentration is not seen because high-enough fluences cannot be reached within a reasonable computing time. This is also the reason why larger particle sizes could not be studied.

The sputtering yield was determined for clusters of 400–2000 atoms from 1000 independent irradiation events for each particle size. The obtained value of about 0.3 is consistent with our previous finding.[11] However, surprisingly the yield does not vary in this size range. This is in stark contrast to heavy ion irradiation that shows a strong dependence on the particle size.[8] This is because sputtering by light ions is mainly due to single knock-on atoms, while for heavier ions linear cascades dominate.[16] The linear cascade's extent and its interaction with the particle surface leads to the size dependence observed for heavy ions.[8] Since this interaction is missing in single knock-on sputtering, the size dependence is absent.

Figure 2 shows the maximal vacancy concentrations obtained from the simulations. For small particles the vacancy concentration is small because vacancy clusters connected to the surface are interpreted as surface roughness by our analysis. As the particle size grows, however, the maximal concentration exceeds that for bulk platinum, for which a value of 4.3% was obtained. The reason for this is that, contrary to bulk, the interstitial component of the irradiation-induced Frenkel pair is able to escape from the particle, causing a supersaturation of vacancies.

To understand the sputtering and evolution of the vacancy concentration, we construct a simple rate equation model to follow the number of vacancies and the number of atoms in the particle during irradiation. The inset of Fig. 1 depicts the processes involved in the model and the main assumptions are the following.

The particle is assumed to be spherical, the number of atoms for an fcc metal cluster thus being $n_{\mathrm{at}}=\frac{16\pi r^3}{3a^3}$, where r is the particle radius and a is the lattice constant. To separate bulk and surface damage, surface atoms are defined to be those with a distance of less than $4r_{\mathrm{at}}$ from the surface, where r_{at} is the atomic radius taken as half of the nearest-neighbor distance. Because a particle's surface roughness increases considerably with irradiation, the choice of the depth of the surface layer, which determines the fraction of surface atoms, is not obvious. Although not a critical factor in the model, it was adjusted for best correspondence between the model and simulations.

The incoming ions are assumed to create damage according to the Kinchin-Pease relation.[17,18] The most often used form is $Y_d=\kappa\frac{E}{2E_d}$, where E is the deposited energy, E_d is the threshold displacement energy, and κ is the damage efficiency usually taken to be 0.8.[18] We do not here include the efficiency function, $\xi(E)$, since at the presently relevant recoil energies (see below), $\xi(E)\approx 1$.[19] The above formula, however, applies for $E\in[2E_d,E_1]$, where E_1 is the threshold above which only electronic stopping is taken into account. For energies lower than $2E_d$, the Kinchin-Pease formula gives 0 or 1, below and above E_d, respectively. As the deposited energies in the present case are below $2E_d$ (see below), the low-energy regime applies. We make the simplest approximation and linearize the low-energy part ($E<2E_d$) thus giving $Y_d=\frac{E}{2E_d}$. Note that this corresponds to the higher-energy part with $\kappa=1$.

Further, the damage created according to the Kinchin-Pease model is divided between surface and bulk atoms, so that the number of Frenkel pairs created by an incoming ion is $Y_d f$, f being the fraction of bulk atoms. Correspondingly, $Y_{ds}(1-f)$ gives the number of Frenkel pairs created at the surface, Y_{ds} containing the threshold displacement energy for surface atoms E_{ds}.

The deposited energy per impacting ion, E, was determined as follows. A nuclear stopping of 1.526 eV/Å for 3 keV He in Pt was obtained from a SRIM (Ref. 20) calculation. The range an ion travels through a spherical particle is, averaged over the particle cross section, $\frac{4}{3}r$. From these, the average deposited energy was calculated based on the num-

ber of atoms in the particle. For 400–4000 atom particles the average deposited energy is around 25–50 eV.

The threshold displacement energies were obtained by simulating recoils starting from lattice sites in random directions. First an atom was selected near the center of the cell, and a three-dimensional random direction was selected. For each atom and direction, the recoil was simulated at an increasing energy with steps of 2 eV until a stable defect was formed. Details of the procedure are given in Ref. 21. An average value of E_d=91 eV was obtained. We also calculated the average threshold energy for sputtering using the same procedure, but picking only the top layer atoms on a (100) or (111) surface as the initial recoil. We obtained surface threshold energies (E_{ds}) for sputtering of 63 ± 3 eV for the (100) surface and 66 ± 4 eV for (111) surface, i.e., an average of 64.5 eV. We note that these average thresholds are rather high because many recoils are directed in toward the bulk—the minimum threshold energy for sputtering was of course much lower, ~10 eV.

Recombination effects were taken into account by assuming that an athermal/ballistic interstitial (from a Frenkel pair created in the bulk) going through the particle has on average $n_{\text{site}}=r/(2r_{\text{at}})$ possible sites to recombine with a vacancy. At a single site, the recombination probability is $P_{\text{site}}=\frac{n_{\text{vac}}V_{\text{rec}}}{n_{\text{at}}V_{\text{at}}}$, where n_{vac} is the number of vacancies. V_{rec} is the recombination volume of a vacancy assumed to be a sphere of radius $r_{\text{rec}}=k_r r_{\text{at}}$. The total recombination probability thus becomes $P_R=1-(1-P_{\text{site}})^{n_{\text{site}}}$. In addition, we assume that a fraction f_Θ of recoiled surface atoms contribute to vacancy recombination. This factor also emulates the effect of recombination induced by subthreshold recoils.

Using these assumptions, the following kinetic equations can be written as

$$\frac{dn_{\text{vac}}}{dn_i} = Y_d f(1-P_R) - \left(-\frac{dn_{\text{at}}}{dn_i}V_{\text{at}}\right)\frac{n_{\text{vac}}}{n_{\text{at}}V_{\text{at}}},$$

$$-Y_{ds}(1-f)f_\Theta P_R,$$

$$\frac{dn_{\text{at}}}{dn_i} = -Y_d f(1-P_R) - Y_{ds}(1-f)(1-f_\Theta P_R). \qquad (1)$$

Above, n_i is the number of impacting ions. Introducing the equations term by term, the first term in the first equation gives the number of bulk vacancies created per impacting ion. The value from the Kinchin-Pease relation is modified by the probability P_R that an interstitial will recombine with an already existing vacancy before leaving the particle. The second term gives the loss of vacancies due to the shrinking of the particle, given by the disappearing volume/impacting ion multiplied with the vacancy concentration. The last term is the contribution of recoiled surface atoms to vacancy recombination. The second equation gives the number of sputtered bulk and surface atoms, the latter modified by the fraction f_Θ.

After the assumptions listed above the model contains two free parameters, the radius of the recombination volume and the fraction of surface recoils contributing to vacancy recombination. The former was adjusted to $r_{\text{rec}}=1.55r_{\text{at}}=2.15$ Å to get correspondence to the simulation results. This is in quite a good agreement with Ref. 22, where a value of $1.84r_{\text{at}}=1.4$ Å was obtained for diamond, a material very different from platinum. For the fraction of surface recoils contributing to vacancy recombination we got $f_\Theta=0.1$, which is a very reasonable result.

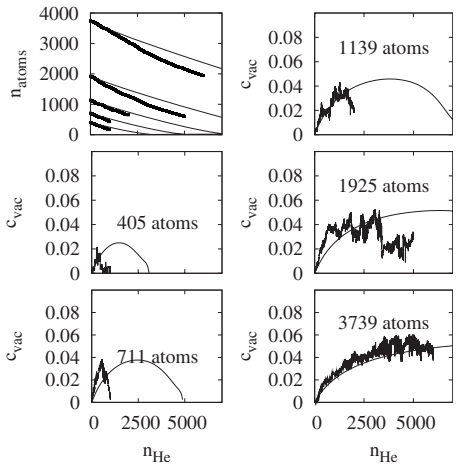

FIG. 3. Number of vacancies and atoms as a function of helium fluence for particles of different sizes. The smooth thin lines show the results from the analytical model.

The results of the simulations and the model are compared in Fig. 3 that shows the number of atoms and vacancy concentration in each particle size as a function of helium fluence. Figure 2 shows the maximum concentrations at sizes at which 90% of $c_{\text{vac}}^{\text{max}}$ is reached, as the concentration in the larger particles rises very slowly after this. The model tends to somewhat overestimate the fluence at which the maximum vacancy content is reached. The decrease in the number of atoms is predicted quite well, although at least at higher fluences sputtering is slightly underestimated. This may be partly due to the model ignoring changes in surface roughness and contributes to the overestimation of the fluence needed to obtain the maximal vacancy concentration. However, given the simplicity of the model, the overall correspondence is quite good. The qualitative features of damage accumulation are also very well reproduced, allowing an understanding of the contributing processes.

Our results show that at these sizes, the maximum vacancy concentration is an increasing function of the particle size. To explore the limits of vacancy concentration obtainable with irradiation, we also ran simulations, where instead of simulating the incoming helium ion explicitly, an energy of 100 eV was given directly to a random cluster atom in a random direction. For the ~5 nm, 3739 atom particles, concentrations as high as ~10% were obtained. While this does not directly correspond to realistic irradiation conditions, it gives an idea of what kind of concentrations may be possible to be achieved with other irradiation parameters. The simulations without the explicit helium were also used to confirm the rising trend in vacancy concentration with the particle size.

In conclusion, we have applied a simple rate equation model to simulations of 3 keV He irradiation of Pt nanoparticles. The model fits the nanoparticles' response very rea-

sonably and provides an intuitive picture of the single knock-on processes occurring during irradiation, allowing for estimating similar behavior in other materials. We find that in contrast to heavier ions,[8] the sputtering yield does not depend on the particle size, the reason being the nature of single knock-on vs linear cascade sputtering. In contrast, very high vacancy concentrations can be obtained in nanoparticles, and the maximal concentration depends on the particle size. This is to be contrasted with the thermodynamic equilibrium concentration that is lower in nanoparticles than bulk.[23] A supersaturation of vacancies has in fact been proposed to be a significant factor in increasing the susceptibility to amorphization of alloyed nanoparticles in Ref. 3, where it was shown that FePt and CuAu nanoparticles amorphize although the bulk alloys do not.

This work was done within the Finnish Centre of Excellence in Computational Molecular Science (CMS), financed by the Academy of Finland and the University of Helsinki. We also gratefully acknowledge support within an exchange program from the Academy of Finland and the German Foreign Exchange Service (DAAD), as well as the grants of computer time from CSC, the Finnish IT Center for Science.

*tommi.jarvi@iki.fi

[1] U. Wiedwald, A. Klimmer, B. Kern, L. Han, H.-G. Boyen, P. Ziemann, and K. Fauth, Appl. Phys. Lett. **90**, 062508 (2007).
[2] O. Dmitrieva, B. Rellinghaus, J. Kästner, M. O. Liedke, and J. Fassbender, J. Appl. Phys. **97**, 10N112 (2005).
[3] T. T. Järvi, D. Pohl, K. Albe, B. Rellinghaus, L. Schultz, J. Fassbender, A. Kuronen, and K. Nordlund, EPL **85**, 26001 (2009).
[4] D. Pohl, E. Mohn, B. Rellinghaus, J. Fassbender, and L. Schultz (unpublished).
[5] K. Meinander and K. Nordlund, Phys. Rev. B **79**, 045411 (2009).
[6] E. M. Bringa and R. E. Johnson, Nucl. Instrum. Methods Phys. Res. B **193**, 365 (2002).
[7] A. V. Krasheninnikov and K. Nordlund (unpublished).
[8] T. T. Järvi, J. A. Pakarinen, A. Kuronen, and K. Nordlund, EPL **82**, 26002 (2008).
[9] S. Zimmermann and H. M. Urbassek, Int. J. Mass Spectrom. **272**, 91 (2008).
[10] R. Kissel and H. M. Urbassek, Nucl. Instrum. Methods Phys. Res. B **180**, 293 (2001).
[11] T. T. Järvi, A. Kuronen, K. Nordlund, and K. Albe, J. Appl. Phys. **102**, 124304 (2007).
[12] M. Müller, P. Erhart, and K. Albe, Phys. Rev. B **76**, 155412 (2007).
[13] J. F. Ziegler, J. P. Biersack, and U. Littmark, *The Stopping and Range of Ions in Matter* (Pergamon, New York, 1985).
[14] M. Müller, Ph.D. thesis, Technische Universität Darmstadt, 2007.
[15] P. Ehrhart, *Landolt-Börnstein: Numerical Data and Functional Relationships in Science and Technology, 25* (Springer-Verlag, Heidelberg, 1991).
[16] P. Sigmund, in *Sputtering by Particle Bombardment I*, Topics in Applied Physics Vol. 47, edited by R. Behrisch (Springer-Verlag, Heidelberg, 1981), Chap. 2, pp. 9–71.
[17] G. Kinchin and R. Pease, Rep. Prog. Phys. **18**, 1 (1955).
[18] M. J. Norgett, M. T. Robinson, and I. M. Torrens, Nucl. Eng. Des. **33**, 50 (1975).
[19] R. S. Averback and T. Diaz de la Rubia, in *Solid State Physics*, edited by H. Ehrenfest and F. Spaepen (Academic, New York, 1998), Vol. 51, pp. 281–402.
[20] J. F. Ziegler, SRIM-2008 software package available online at www.srim.org.
[21] K. Nordlund, J. Wallenius, and L. Malerba, Nucl. Instrum. Methods Phys. Res. B **246**, 322 (2006).
[22] J. F. Prins, J. Phys. D **34**, 3003 (2001).
[23] M. Müller and K. Albe, Acta Mater. **55**, 3237 (2007).